

# Optimal Sensor and Actuator Scheduling in Sampled-Data Control of Spatially Distributed Processes<sup>\*</sup>

Da Xue and Nael H. El-Farra<sup>\*</sup>

<sup>\*</sup> *University of California, Davis, CA 95616 USA (e-mail:  
nhelfarra@ucdavis.edu)*

---

**Abstract:** This work presents an optimization-based methodology for the placement and scheduling of measurement sensors and control actuators in spatially-distributed processes with low-order dynamics and discretely-sampled output measurements. Initially, a sampled-data observer-based controller, with an inter-sample model predictor, is designed based on an approximate finite-dimensional system that captures the infinite-dimensional system's dominant dynamics. An explicit characterization of the interdependence between the stabilizing locations of the sensors and actuators and the maximum allowable sampling period is obtained. Based on this characterization, a constrained finite-horizon optimization problem is formulated to obtain the sensor and actuator locations, together the corresponding sampling period, that optimally balance the tradeoff between the control performance requirements on the one hand, and the demand for reduced sampling, on the other. The objective function penalizes both the control performance cost, expressed in terms of the response speed and the control effort, and the sampling cost, expressed in terms of the sampling frequency. The optimization problem is solved in a receding horizon fashion, leading to a dynamic policy that varies the sensor and actuator spatial placement, together with the sampling period, over time. The developed methodology is illustrated through an application to a simulated diffusion-reaction process example.

*Keywords:* Sampled-data control, sensor and actuator placement, receding horizon optimization, scheduling, spatially-distributed systems.

---

## 1. INTRODUCTION

Despite the extensive body of research work on control of spatially-distributed systems, the problem of designing sampled-data feedback controllers for spatially-distributed processes has received relatively limited attention (e.g., see Logemann et al. (2005); Cheng et al. (2009); Fridman and Blichovsky (2010) for some notable exceptions). This is an important problem given the prevalent use of digital sensors and controllers in industrial control systems. To date, the overwhelming majority of studies on the analysis and design of sampled-data control systems have focused primarily on lumped parameter systems modeled by ordinary differential equations (e.g., see Chen and Francis (1995); Netic and Grune (2005); Hu et al. (2007); Naghshtabrizi et al. (2008); Fujioka (2009); Hu and El-Farra (2011)).

An effort to address the sampled-data control problem for spatially-distributed systems was undertaken in a series of earlier works (e.g., Yao and El-Farra (2011, 2012)). The main idea was to include an approximate finite-dimensional model of the infinite-dimensional system in the controller to provide estimates of the dominant slow states that compensate for the unavailability of output measurements between sampling times, and to update the model states using the actual measurements at each sampling time. A key objective of this model-based control ap-

<sup>\*</sup> Financial support by NSF, CBET-1438456, is gratefully acknowledged.

proach was to guarantee closed-loop stability with minimal sampling frequency. This is an appealing goal in situations where technological constraints on the measurement sensing techniques make it difficult or costly to collect measurements frequently. To this end, an exact characterization of the maximum allowable sampling period required for stabilization was obtained in the earlier studies and found to depend on the spatial placement of the measurement sensors and control actuators. An implication of this finding is that one could use this characterization to identify the set of feasible sensor and actuator locations that can achieve stabilization with minimal sampling frequencies. While this is important from a sampling cost savings standpoint, the resulting actuator and sensor placement does not consider the impact of discrete measurement sampling on closed-loop performance. It is well known, for example, that faster sampling rates are typically required to enhance the control system performance. Ultimately, there is a need to resolve the inherent conflict that arises between the tight restrictions on sampling rates which are required to maintain the control system performance on the one hand, and the usual demand for limited sampling frequency which is desired to minimize measurement costs.

Motivated by these considerations, we present in this work an optimization-based approach for the integration of control and actuator/sensor scheduling in spatially-distributed processes with discretely-sampled output measurements. The objective is to simultaneously optimize

the control system performance and the sampling costs by dynamically scheduling the sensor and actuator locations, as well as the sampling period, subject to the appropriate stability constraints. The rest of the paper is organized as follows. Following some preliminaries in Section 2, an observer-based controller that relies on an inter-sample model predictor and a fixed sensor-actuator placement is introduced in Section 3, along with a parametric characterization of its closed-loop stability region. This characterization is incorporated as a constraint within a finite-horizon optimization problem that is formulated in Section 4, where the cost function includes explicit penalties on the response speed, the control action and the sampling frequency. A receding horizon strategy for implementing the optimization problem solution is then devised in Section 5 to determine the optimal placement and scheduling of the sensors and actuators and the optimal sampling rate. Finally, a simulation case study is presented in Section 6.

## 2. PRELIMINARIES

We consider spatially-distributed processes modeled by highly-dissipative infinite-dimensional systems. An example of this class of systems, which is introduced in this section to illustrate the subsequent theoretical development, are systems described by parabolic PDEs:

$$\begin{aligned} \frac{\partial \bar{x}}{\partial t} &= \alpha \frac{\partial^2 \bar{x}}{\partial z^2} + \beta \bar{x} + \omega \sum_{i=1}^n b_i(z) u_i \\ y_i(t) &= \int_0^\pi q_i(z) \bar{x}(z, t) dz, \quad i \in \{1, 2, \dots, l\} \end{aligned} \quad (1)$$

subject to the boundary and initial conditions:

$$\bar{x}(0, t) = \bar{x}(\pi, t) = 0, \quad \bar{x}(z, 0) = \bar{x}_0(z) \quad (2)$$

where  $\bar{x}(z, t) \in \mathbb{R}$  is the process state variable,  $z \in [0, \pi]$  is the spatial coordinate,  $t \in [0, \infty)$  is the time,  $u_i \in \mathbb{R}$  is the  $i$ -th manipulated input,  $n$  is the number of manipulated inputs,  $b_i(\cdot)$  is the actuator distribution function,  $y_i$  is the  $i$ -th measured output,  $q_i(\cdot)$  is the  $i$ -th sensor distribution function, and  $\bar{x}_0(z)$  is a smooth function of  $z$ . The PDE of (1), subject to the boundary and initial conditions of (2) can be formulated as an infinite-dimensional system with the following state-space representation:

$$\begin{aligned} \dot{x}(t) &= \mathcal{A}x(t) + \mathcal{B}u(t), \quad x(0) = x_0 \\ y(t) &= \mathcal{Q}x(t) \end{aligned} \quad (3)$$

where  $x(t) = \bar{x}(z, t)$ ,  $t > 0$ ,  $z \in [0, \pi]$ , is the state function defined on an appropriate Hilbert space,  $\mathcal{H} = L_2(0, \pi)$ , endowed with the proper inner product and norm;  $\mathcal{A}$  is the differential operator;  $\mathcal{B}$  and  $\mathcal{Q}$  are the input and output operators, respectively;  $u = [u_1 \dots u_n]^T$ ,  $y = [y_1 \dots y_l]^T$ , and  $x_0 = \bar{x}_0(z)$ . Applying modal decomposition techniques, the infinite-dimensional system can be decomposed as follows:

$$\dot{x}_s = \mathcal{A}_s x_s + \mathcal{B}_s u, \quad x_s(0) = \mathcal{P}_s x_0 \quad (4)$$

$$\dot{x}_f = \mathcal{A}_f x_f + \mathcal{B}_f u, \quad x_f(0) = \mathcal{P}_f x_0 \quad (5)$$

$$y = \mathcal{Q}_s x_s + \mathcal{Q}_f x_f \quad (6)$$

where  $x_s = \mathcal{P}_s x$  is the state of a finite-dimensional system that describes the evolution of the slow (possibly unstable) eigenmodes;  $x_f = \mathcal{P}_f x$  is the state of an infinite-dimensional system that captures the evolution of the fast (stable) eigenmodes; and  $\mathcal{P}_s$  and  $\mathcal{P}_f$  are the orthogonal projection operators, where  $\mathcal{A}_s = \mathcal{P}_s \mathcal{A}$ ,  $\mathcal{B}_s = \mathcal{P}_s \mathcal{B}$ ,  $\mathcal{A}_f = \mathcal{P}_f \mathcal{A}$ , and  $\mathcal{B}_f = \mathcal{P}_f \mathcal{B}$ . To simplify the presentation of the

main results, we assume that the number of actuators and sensors is the same and equal to the number of the dominant modes (i.e.,  $n = l = m$ ).

Based on the above decomposition, the following approximate finite-dimensional system which describes the temporal evolution of the slow (possibly unstable) eigenmodes can be derived using Galerkin's method:

$$\dot{a}_s = A_s a_s + B_s(z_a) u(t), \quad \bar{y}_s = Q_s(z_s) a_s \quad (7)$$

where  $a_s = [a_1 \dots a_m]^T \in \mathbb{R}^m$ ;  $a_i$  is the amplitude of the  $i$ -th eigenmode;  $\bar{y}_s$  is the output;  $A_s$  is an  $m \times m$  diagonal matrix of the form  $A_s = \text{diag}\{\lambda_j\}$  containing the slow eigenvalues in the spectrum of  $\mathcal{A}$ ;  $B_s$  is an  $m \times m$  input matrix whose individual elements are parameterized by the locations of the control actuators  $z_a$ ;  $Q_s$  is an invertible  $m \times m$  output matrix whose individual elements are parameterized by the locations of the measurement sensors  $z_s$  (the invertibility assumption can be ensured by proper selection of the sensors' locations). The reduced-order system of (7) will be used in the next section to design a model-based output feedback controller that achieves stabilization using discretely-sampled output measurements.

## 3. OBSERVER-BASED CONTROL USING AN INTER-SAMPLE MODEL PREDICTOR

We consider an output-feedback control structure in which the output measurements collected by the sensors are available to the controller only at discrete sampling times. A dynamic state observer is used to generate an estimate of the state which is used to compute the control action. Owing to the unavailability of output measurements between sampling times, an inter-sample model predictor is used to generate an estimate of the output between sampling times. This estimate is used by the observer and is re-set using the actual output when it becomes available at the next sampling time. The implementation of this combined control and update strategy is given by:

$$\begin{aligned} u(t) &= K\eta(t), \quad t \in [t_k, t_{k+1}) \\ \dot{\eta}(t) &= \hat{A}_s \eta(t) + \hat{B}_s u(t) + L(\hat{y}_s(t) - \hat{Q}_s \eta(t)) \\ \hat{a}_s(t) &= \hat{A}_s \hat{a}_s(t) + \hat{B}_s(z_a) u(t) \\ \hat{y}_s(t) &= \hat{Q}_s(z_s) \hat{a}_s(t) \\ \hat{a}_s(t_k) &= \hat{Q}_s^{-1} \bar{y}_s(t_k), \quad k \in \{1, 2, \dots\} \\ t_{k+1} &= t_k + \Delta \end{aligned} \quad (8)$$

where  $\eta$  is the state of the observer;  $\hat{A}_s$ ,  $\hat{B}_s$  and  $\hat{Q}_s$  are approximate models of  $A_s$ ,  $B_s$  and  $Q_s$ , respectively;  $K$  and  $L$  are the feedback controller and observer gains, respectively;  $\hat{a}_s$  and  $\hat{y}_s$  are the state and output of the inter-sample model predictor;  $t_k$  denotes the  $k$ -th sampling time, and  $\Delta > 0$  is the sampling period. For simplicity, we assume that  $\hat{Q}_s = Q_s$  (i.e., no uncertainty in  $z_s$ ).

The following theorem provides an exact characterization of the closed-loop stability properties under the observer-based controller of (8) with a periodic sampling strategy. The proof is conceptually similar to the one in Garcia et al. (2014) and is omitted for brevity.

*Theorem 1.* Referring to the closed-loop system of (7)-(8), the origin is exponentially stable if and only if:

$$\lambda_{\max}[M(K, L, \Delta, \hat{A}_s, \hat{B}_s(z_a), A_s, B_s, \hat{Q}_s(z_s))] < 1, \quad (9)$$

where  $\lambda_{\max}$  is the largest eigenvalue magnitude of the matrix  $M$  which is given by:

$$M = I_s e^{\Lambda \Delta} I_s, \quad (10)$$

where

$$I_s = \begin{bmatrix} I_{m \times m} & O_{m \times m} & O_{m \times m} \\ O_{m \times m} & I_{m \times m} & O_{m \times m} \\ O_{m \times m} & O_{m \times m} & O_{m \times m} \end{bmatrix} \quad (11)$$

where  $I_{m \times m}$  is the  $m \times m$  identity matrix,  $O_{m \times m}$  is the  $m \times m$  zero matrix, and  $\Lambda$  is the closed-loop matrix given by:

$$\Lambda = \begin{bmatrix} A_s & B_s K & O_{m \times m} \\ L \hat{Q}_s & \hat{A}_s + \hat{B}_s K - L \hat{Q}_s & -L \hat{Q}_s \\ (A_s - \hat{A}_s) & (B_s - \hat{B}_s) K & \hat{A}_s \end{bmatrix} \quad (12)$$

*Remark 1.* The stability condition of (9) provides an explicit characterization of the interdependence between the process and model parameters, the controller and observer gains, the sampling period, and the sensor and actuator locations in influencing closed-loop stability. For example, for fixed model and controller parameters, this characterization can be used to determine how the maximum allowable sampling period depends on the spatial placement of the sensors and actuators. This characterization is important as it provides the basis for the optimization formulation introduced in the next section.

#### 4. AN OPTIMIZATION-BASED FORMULATION FOR SENSOR AND ACTUATOR PLACEMENT

While the stability condition in Theorem 1 provides a useful tool that can be used to analyze how different sensor and actuator locations influence the size of the maximum allowable sampling period, it leaves open the question of how to best place the sensors and actuators in a way that optimally balances the desire for reduced sampling frequency with the demand for improved control system performance. Furthermore, the implementation of the observer-based controller of (8) involves the use of a constant sampling rate which is not always the best choice, especially in the presence of unexpected external disturbances and changing operating conditions. In this section and the next, we describe an optimization-based formulation that aims to address both problems.

We consider the following finite-horizon optimization problem in which the sampling period, the sensor and actuator locations at any given time are determined by minimizing the following cost functional:

$$\min_{z_s^k, z_a^k, \Delta_k} J(z_s^k, z_a^k, \Delta_k)$$

$$\text{where, } J = J_p + J_s$$

$$J_p = \int_{t_k}^{t_k+H} [\hat{y}_s^T(\tau) W_y \hat{y}_s(\tau) + u^T(\tau) W_u u(\tau)] dt$$

$$J_s = \int_{t_k}^{t_k+H} \beta(\Delta_k, w_\Delta) dt$$

subject to:

$$\hat{y}_s(t) = \hat{Q}_s(z_s^k) \hat{a}_s(t), \quad t_k \leq t < t_k + H$$

$$\hat{a}_s(t) = \hat{A}_s \hat{a}_s(t) + \hat{B}_s(z_a^k) u(t), \quad t_k \leq t < t_k + H$$

$$\dot{\eta}(t) = \hat{A}_s \eta(t) + \hat{B}_s(z_a^k) u(t) + L(\hat{y}_s(t) - \hat{Q}_s(z_s^k) \eta(t)), \\ t_k \leq t < t_k + H$$

$$u(t) = K \eta(t), \quad t_k \leq t < t_k + H$$

$$\lambda_{\max}[M(K, L, \Delta_k, \hat{A}_s, \hat{B}_s, A_s, B_s, \hat{Q}_s)] < 1$$

(13)

where  $M$  is defined in (10)-(12),  $t_k$ , is the  $k$ -th sampling time,  $z_s^k \triangleq z_s(t_k)$ ,  $z_a^k \triangleq z_a(t_k)$ ,  $H$  denotes the optimization horizon,  $W_y$ ,  $W_u$  are positive-definite weighting matrices that represent the penalties on the model output and the control action, respectively, and  $\beta(\Delta_k, w_\Delta) > 0$  is the penalty on the sampling frequency, which is taken to be a smooth function of the sampling period  $\Delta_k$ , and  $w_\Delta$  is a positive weighting on the sampling penalty.

Referring to the above optimization formulation, the decision variables are the sensor locations,  $z_s^k$ , the actuator locations  $z_a^k$ , and the sampling period,  $\Delta_k$ , which must be chosen at time  $t_k$  to satisfy the closed-loop stability condition of (9), which captures the feasible region for the optimization problem. The solution to the optimization problem at a given time  $t_k$  yields the optimal triple  $(z_s^k, z_a^k, \Delta_k)$  that minimizes the total cost  $J$  over the given horizon  $H$ .

*Remark 2.* While the optimal actuator/sensor placement problem for spatially-distributed systems has been the subject of significant prior work (e.g., see Antoniadis and Christofides (2000); Demetriou and Kazantzis (2004); Armaou and Demetriou (2006); Iftime and Demetriou (2009)), the emphasis of previous approaches has been either on meeting certain controllability and observability requirements, or on optimizing the performance of the closed-loop system (e.g., in terms of the response speed and control effort) without consideration of the effects or costs associated with discrete measurement sampling. The formulation proposed in (13) represents a departure from conventional approaches by aiming to balance control performance considerations with the demand for reduced sampling. Specifically, the objective function in (13) consists of a performance cost,  $J_p$ , which imposes penalties on the model output and the control action, and a sampling cost,  $J_s$ , which penalizes frequent sampling. A simple choice for the sampling cost is to set  $\beta = w_\Delta / \Delta$ , which ensures that faster sampling rates incur larger penalties. Note that  $J_p$  is expressed in terms of the model output since the actual output is unavailable between sampling times.

*Remark 3.* The choice of the various penalty weights in the optimization formulation should be made to reflect the relative significance of the different costs. For example, imposing larger penalties on the sampling frequency suggests an increased emphasis on the sampling cost relative to the control performance. On the other hand, for systems where sampling costs are negligible, more emphasis is placed on the controller performance.

#### 5. DYNAMIC ACTUATOR/SENSOR SCHEDULING USING RECEDING HORIZON OPTIMIZATION

Referring to the implementation of the optimization formulation in (13), one possible strategy is to solve the problem once at the beginning of the horizon, apply the resulting optimal sensor and actuator locations and sampling period over the entire horizon length, and then repeat the optimization when the end of the horizon is reached. While this strategy reduces the computational load associated with repeated on-line optimization (especially if  $H$  is large), it does not take into account the fact that the cost function is dependent on the model state trajectory, and the fact that the model state is to be updated at each

sampling time. It may also limit the ability of the process to respond in a timely fashion to changes in operating conditions by limiting the frequency of feedback from the process. These considerations call for a receding horizon implementation strategy, where (13) is solved on-line at each  $t_k$ , and the resulting sensor and actuator locations,  $z_s^k$  and  $z_a^k$ , together with the corresponding stabilizing sampling period,  $\Delta_k$ , are implemented only for a single sampling period within the horizon. By the end of the sampling interval at  $t = t_k + \Delta_k^*$ , a new sampled output measurement is sent from the sensor to the controller and used to update the model state as follows:

$$\begin{aligned} (z_s(t), z_a(t), \Delta(t)) &= (z_s^{k*}, z_a^{k*}, \Delta_k^*) \\ &= \arg \min_{z_s^k, z_a^k, \Delta_k} J, \quad \forall t \in [t_k, t_k + \Delta_k^*) \\ \hat{a}_s(t_k + \Delta_k^*) &= \hat{Q}_s^{-1}(z_s^{k*})\bar{y}_s(t_k + \Delta_k^*) \end{aligned}$$

With the updated model state, the optimization problem of (13) is re-solved to determine  $(z_s^{k+1*}, z_a^{k+1*}, \Delta_{k+1}^*)$  at  $t = t_{k+1} = t_k + \Delta_k^*$ . The newly obtained solution is then implemented for  $t \in [t_{k+1}, t_{k+1} + \Delta_{k+1}^*)$  and the problem is re-solved at end of the sampling period. Algorithm 1 summarizes the on-line receding horizon strategy.

*Remark 4.* The repeated on-line optimization approach described in Algorithm 1 leads to a time-varying schedule for moving the sensor and actuator locations as well as the sampling rate. Compared with the observer-based controller in (8) with a constant sampling rate, the time-varying scheduled sensor and actuator locations and sampling rates obtained through the optimization formulation allow the process to adaptively respond to unexpected changes in operating conditions.

*Remark 5.* The receding horizon implementation of the optimization formulation bears resemblance to the implementation of MPC policies, where a finite-horizon optimization problem is re-solved at every sampling time, and the optimal solution is implemented for the duration of the first sampling period only, at the end of which new output measurements are obtained and fed back to the controller to update the model state and correct possible deviations in the model state trajectory. This feedback-based approach is appealing since it provides some robustness to process-model mismatch and changes in operating conditions due to disturbances. Note, however, that unlike conventional MPC schemes, the frequency at which the optimization problem is re-solved is not fixed. It is rather determined online as part of the optimization problem solution. Furthermore, closed-loop stability is guaranteed through the constraint in (9) and is therefore independent of the horizon length.

*Remark 6.* From an implementation standpoint, the horizon length should be chosen such that  $H > \Delta$ . A suitable choice for  $H$  can be made on the basis of the characterization of the feasible region in terms of  $z_a, z_s$  and  $\Delta$  obtained prior to online implementation. Specifically, by analyzing the  $\lambda_{\max}(M)$  over a specified range of sensor and actuator locations, an upper bound on the feasible sampling period can be obtained. In other words, the maximum allowable sampling period,  $\Delta_{\max}$ , can be viewed as a function of  $z_s$  and  $z_a$ , where the stability condition that  $\lambda_{\max}(M) < 1$  is satisfied. Then by considering a range of possible sensor and actuator locations, a corresponding range of possible sampling periods could be estimated and used to choose

- 1 **characterize**  $\Delta_{\max}(z_s, z_a)$  based on the stability condition of (9);
- 2 **specify** the penalty weights  $W_y, W_u$  and  $w_\Delta$ ;
- 3 **initialize**  $\hat{y}_s(t_0) = \bar{y}_s(t_0), \hat{a}_s(t_0) = \eta(t_0) = \hat{Q}_s^{-1}\bar{y}_s(t_0)$ ;
- 4 **solve** (13) to determine  $z_s^0, z_a^0$ , and  $\Delta_0$ ;
- 5 **place**  $z_s = z_s^0$  and  $z_a = z_a^0$ ;
- 6 **start** system operation;
- 7 **sample** output measurements  $\bar{y}_s(t)$  at  $t = \Delta_1$ ;
- 8 **set**  $k = 1$ ;
- 9 **solve** equation (13) to determine  $z_s^k, z_a^k$  and  $\Delta_k$ ;
- 10 **relocate**  $z_s = z_s^k$  and  $z_a = z_a^k$ ;
- 11 **while**  $t_k \leq t < t_k + \Delta_k$  **do**
  - $z_s(t) = z_s^k$  and  $z_a(t) = z_a^k$ ;
  - $u(t) = K(\eta(t))$ ;
- end**
- 12 **if**  $t = t_k + \Delta_k$  **then**
  - sample** output measurements  $\bar{y}_s(t)$ ;
  - update** model state  $\hat{a}_s(t) = \hat{Q}_s^{-1}\bar{y}_s(t)$ ;
  - $k = k + 1$ ;
  - goto** step 9
- end**

**Algorithm 1.** A receding horizon implementation strategy for actuator/sensor scheduling.

a suitable horizon length, where  $\Delta_{\max}$  serves as a lower bound on  $H$  (see Section 6 for an analysis of the impact of the horizon length).

## 6. SIMULATION EXAMPLE

We consider a non-isothermal diffusion-reaction process described by the following parabolic PDE:

$$\frac{\partial \bar{x}}{\partial t} = \frac{\partial^2 \bar{x}}{\partial z^2} + [(\beta_T + \theta_1)\gamma e^{-\gamma} - \beta_U]\bar{x} + \beta_U b(z)u(t) \quad (14)$$

subject to Dirichlet boundary conditions as in (2), where  $\bar{x}$  is a dimensionless process temperature, the manipulating input  $u$  is a dimensionless temperature of the cooling medium,  $\beta_T = 80.0$ ,  $\gamma = 2.0$ ,  $\beta_U = 1.66$  are nominal process parameters,  $\theta_1 = 0.01$  is a parametric uncertainty in the heat of reaction, and  $b(z)$  is the actuator distribution function. It can be verified that the operating steady-state  $x(z, t) = 0$  (with  $u = 0$ ) is unstable. The control objective is to stabilize the temperature profile at this unstable, spatially uniform steady-state by manipulating the temperature of the cooling medium with minimal output measurement sampling. A point control actuator and a single point measurement sensor (with finite support) are assumed to be available. We consider the first eigenvalue of the differential operator to be dominant and use Galerkin's method to derive an uncertain ODE model which is used for the synthesis of the controller. It was verified that the controller under continuous sampling stabilizes the closed-loop system. In the following simulation studies, the controller and observer gains are chosen as  $K = 15$  and  $L = 50$ , respectively.

### 6.1 Characterizing the closed-loop stability region

Following the proposed methodology, the first step is to characterize the stability region in terms of the sensor and

actuator locations and the sampling period. We begin by analyzing the effect of the sensor location on closed-loop stability, the sampling and performance costs when the actuator is placed at the middle of the spatial domain at  $z_a = \pi/2$ .

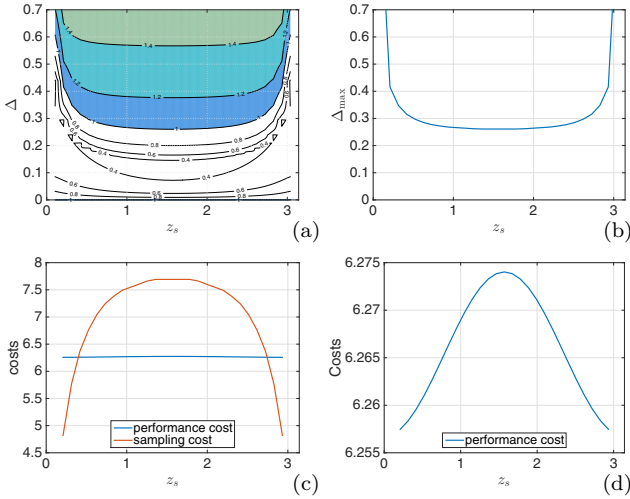


Fig. 1. Plot (a): Contour plot of  $\lambda_{\max}(M(z_s, \Delta))$  for  $z_a = \pi/2$ . Plot (b): Maximum allowable sampling period as a function of sensor location,  $\Delta_{\max}(z_s)$ . Plot (c): Dependence of performance and sampling costs on sensor location. Plot (d): Magnified view of the performance cost as a function of  $z_s$ .

Fig.1(a) shows a contour plot of  $\lambda_{\max}(M(z_s, \Delta))$  where the region enclosed by the unit-contour line (the uncolored region) is the stable region, while the colored region represents the zone where  $\lambda_{\max}(M(z_s, \Delta)) > 1$  and therefore is the unstable region. The implication of this plot is that for a specific sensor location, there is a maximum allowable sampling period beyond which instability would occur. Fig.1(b) traces the unit-contour line in Fig.1(a) which defines the maximum allowable sampling period,  $\Delta_{\max}(z_s)$ , as a function  $z_s$ . The shape of  $\Delta_{\max}(z_s)$  is symmetric and suggests that prolonging the maximum allowable sampling period requires placing the sensor closer to the boundaries.

Fig.1(c) shows a snapshot of the breakdown of the total cost (defined in (13)) at the first sampling time,  $t_1 = 0.208$ , when the optimization problem is solved on-line for the first time in the operating stage. The weighting parameters are chosen as  $W_y = W_u = 150$ ,  $w_\Delta = 1$ , and  $H = 2$  (which is approximately twice the maximum allowable sampling period achievable in the actuator spatial domain). The red line shows the sampling cost,  $J_s$ , as a function of  $z_s$ , while the blue curve depicts the control performance cost,  $J_p$ , as a function of  $z_s$ . As expected, the dependence of  $J_s$  on  $z_s$  is opposite to that of  $\Delta_{\max}(z_s)$  shown in Fig.1(b) since longer sampling periods translate into lower sampling cost. It can be seen that both the sampling and performance costs exhibit similar qualitative dependence on  $z_s$ , where the cost is largest at the center,  $z_s = \pi/2$  and decreases as the sensor is moved closer to the boundary (even though the performance cost appears to depend only weakly on  $z_s$  as can be seen in Fig.1(d)). This suggests that no tradeoff between the two costs exists, and that reducing the total cost favors locating the sensor close to the boundary. This leads to a static (i.e., fixed) sensor placement instead of a dynamic scheduling policy.

Similar to the foregoing analysis, the feasible region with respect to the actuator location can be characterized. Fig.2(a) shows a contour plot of  $\lambda_{\max}(M(z_a, \Delta))$  for a fixed sensor location, whereas Fig.2(b) plots  $\Delta_{\max}(z_a)$  for different sensor locations. The analysis here shows the same trend observed for the sensor placement problem regarding the feasible region, i.e., moving the actuator closer to the boundary helps increase the maximum allowable sampling period (i.e., reduce the sampling cost). Moreover, it can be seen that moving the sensor away from the center enlarges the feasible region leading to longer permissible sampling periods.

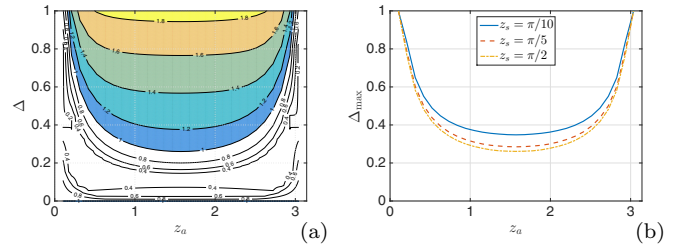


Fig. 2. Plot (a): Contour plot of  $\lambda_{\max}(M(z_a, \Delta, z_s = \pi/2))$ . Plot (b): Maximum allowable sampling period as a function of actuator locations,  $\Delta_{\max}(z_a)$ , for various sensor locations.

### 6.2 Optimization-based actuator scheduling strategy

The stability region characterization in Fig.2 is used in this section to formulate and solve the optimization problem of (13). The weighting parameters and the optimization horizon length are kept the same as in Section 6.1. Note that when the maximum allowable sampling period is used, the closed-loop system is only critically stable. Therefore, to enforce asymptotic stability, the actual sampling period needs to be reduced slightly in practice. In this section, the sampling period used is  $0.7\Delta_{\max}$ .

Fig.3 shows the influence of the actuator location on the total cost and its breakdown at  $t = 0.208$  and at  $t = 4$ , respectively. It can be seen that, in both cases, minimizing the sampling cost favors moving the actuator closer to the boundary whereas minimizing the performance cost favors moving it away from the boundary, leading to an optimal location in between that minimizes the total cost. Comparing the two plots, it can also be seen that the sampling cost does not change over time (note the different scales), whereas the performance cost decreases as time goes on. This is expected since the sampling cost does not depend on the model state, and therefore is unaffected by the sampling and model updates. But since the controller is designed to be stabilizing, the model output continues to decay over time, leading to smaller performance costs. Moreover, at early times when the model output is far away from its steady state, the performance cost is more dominant, but as the output converges, the sampling cost picks up and becomes more dominant at later times. As a result, the shape of the total cost varies over time, causing the optimal actuator location to vary with time.

Fig.4 shows the results when the optimization problem in (13) is solved in a receding horizon fashion. Fig.4(a) depicts the closed-loop state profile when  $z_s = \pi/10$ , while Figs.4(b)-(d) compare the closed-loop state trajectory, the optimal actuator schedules, and the sampling frequencies

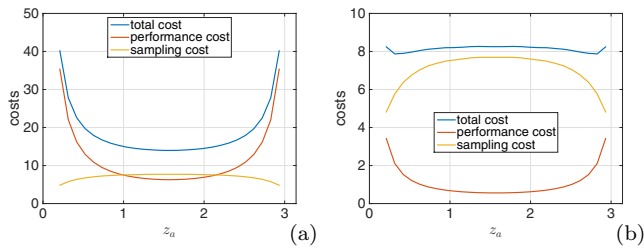


Fig. 3. Snapshots of the sampling cost, the performance cost and the total cost as functions of  $z_a$ , at  $t = 0.208$  (plot (a)) and at  $t = 4$  (plot (b)).

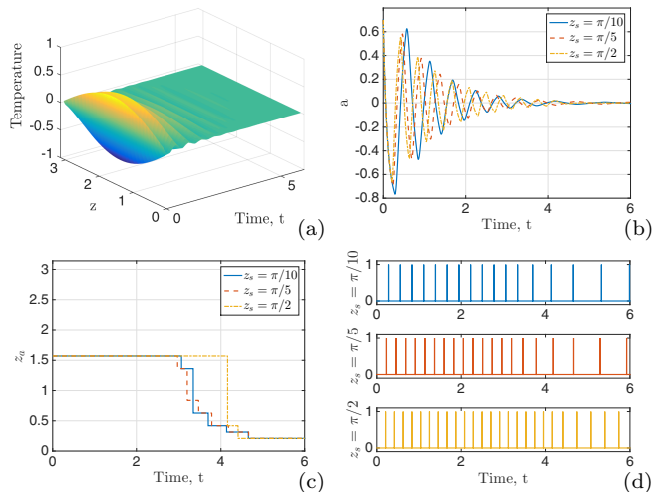


Fig. 4. Plot (a): Closed-loop state profile with  $z_s = \pi/10$ . Plot (b): Comparison of closed-loop state trajectory for various sensor locations. Plot (c): Comparison of the actuator scheduling policies for different sensor locations. Plot (d): Comparison of the sampling times for different sensor locations.

Table 1. Cost comparisons for different sensor locations.

$z_s$	performance cost	sampling cost	total cost
$\pi/2$	2410.2	20.63	2430.8
$\pi/5$	2165.2	16.10	2181.3
$\pi/10$	1865.5	13.60	1879.1

for various sensor locations. Fig.4(b) shows that the sensor location slightly affects the closed-loop state trajectory. However, it does influence the optimal actuator schedule as can be seen in Fig.4(c); and moving the sensor away from the center helps reduce the sampling frequency as can be seen from Fig.4(d). Regarding the optimal actuator schedules, it can be seen from Fig.4(c) that all schedules start at the middle location which is the one that optimizes control performance (recall that the performance cost dominates over the sampling cost initially). However, as the closed-loop state converges close to the steady-state the sampling cost becomes increasingly important, and as a result the actuator location begins to gradually shift closer to the boundary. This transition occurs earlier (with more frequent switchings thereafter) as the sensor is moved closer to the boundary. Table 1 summarizes the cumulative costs (based on the true response over the entire simulation time) for different sensor locations. Placing the sensor at  $z_s = \pi/10$  reduces both the performance and sampling costs, which is consistent with the discussion in Section 6.1.

## REFERENCES

- Antoniades, C. and Christofides, P.D. (2000). Computation of optimal actuator locations for nonlinear controllers in transport-reaction processes. *Comp. & Chem. Eng.*, 24, 577–583.
- Armaou, A. and Demetriou, M. (2006). Optimal actuator/sensor placement for linear parabolic PDEs using spatial  $H_2$  norm. *Chem. Eng. Sci.*, 61, 7351–7367.
- Chen, T. and Francis, B. (1995). *Optimal Sampled-Data Control Systems*. Springer, London; New York.
- Cheng, M., Radisavljevic, V., Chang, C., Lin, C., and Su, W. (2009). A sampled-data singularly perturbed boundary control for a heat conduction system with noncollocated observation. *IEEE Trans. Automat. Contr.*, 54, 1305–1310.
- Demetriou, M. and Kazantzis, N. (2004). Compensation of spatiotemporally varying disturbances in nonlinear transport processes via actuator scheduling. *Int. J. Rob. Nonlin. Contr.*, 14, 191–197.
- Fridman, E. and Blichovsky, A. (2010). Sampled-data stabilization of a class of parabolic systems. In *Proceedings of the 19th International Symposium on Mathematical Theory of Networks and Systems*. Budapest, Hungary.
- Fujioka, H. (2009). A discrete-time approach to stability analysis of systems with aperiodic sample-and-hold devices. *IEEE Trans. Automat. Contr.*, 54, 2440–2445.
- Garcia, E., Antsaklis, P.J., and Montestruque, L.A. (2014). *Model-Based Control of Networked Systems*, Systems & Control: Foundations & Applications. Springer International Publishing, Switzerland.
- Hu, L., Bai, T., Shi, P., and Wu, Z. (2007). Sampled-data control of networked linear control systems. *Automatica*, 43, 903–911.
- Hu, Y. and El-Farra, N.H. (2011). Control, monitoring and reconfiguration of sampled-data hybrid process systems with actuator faults. In *Proceedings of 50th IEEE Conference on Decision and Control*, 3736–3741. Orlando, FL.
- Iftime, O. and Demetriou, M. (2009). Optimal control of switched distributed parameter systems with spatially scheduled actuators. *Automatica*, 45, 312–323.
- Logemann, H., Rebarber, R., and Townley, S. (2005). Generalized sampled-data stabilization of well-posed linear infinite-dimensional systems. *SIAM J. Cont. Optim.*, 44, 1345–1369.
- Naghshabrizi, P., Hespanha, J., and Teel, A. (2008). Exponential stability of impulsive systems with application to uncertain sampled-data systems. *Syst. Contr. Lett.*, 57, 378–385.
- Nesic, D. and Grune, L. (2005). Lyapunov-based continuous-time nonlinear controller redesign for sampled-data implementation. *Automatica*, 41, 1143–1156.
- Yao, Z. and El-Farra, N.H. (2011). Robust fault detection and reconfigurable control of uncertain sampled-data distributed processes. In *Proceedings of 50th IEEE Conference on Decision and Control*, 4925–4930. Orlando, FL.
- Yao, Z. and El-Farra, N.H. (2012). A predictor-corrector approach for multi-rate sampled-data control of spatially distributed systems. In *Proceedings of 51st IEEE Conference on Decision and Control*, 2908–2913. Maui, HI.